Pseudopotential plane-wave study of α-YH_x

Yan Wang and M. Y. Chou
School of Physics, Georgia Institute of Technology, Atlanta, Georgia 30332
(Received 11 November 1993)

The solid-solution phase of hydrogen in hexagonal close-packed yttrium (α-YH_x) is studied using the pseudopotential method within the local-density-functional approximation with a plane-wave basis. The binding energies associated with different interstitial sites are evaluated for several ordered structures: $YH_{0.5}$, $YH_{0.25}$, and $YH_{0.167}$. It is found that the occupation of the tetrahedral site is always energetically favorable. The hydrogen potential-energy curves around the tetrahedral sites along the c axis and along the path connecting the adjacent octahedral sites are also calculated for $YH_{0.25}$. In particular, the local vibrational mode along the c axis is estimated to be 100 meV, in excellent agreement with that measured in neutron-scattering experiments. Finally, the intriguing pairing phenomenon is investigated by calculating the total energy for various pairing configurations. The possibility of pairing between nearest-neighbor tetrahedral sites is excluded due to the high energy. It is found that the pairing of hydrogen across a metal atom is indeed energetically favorable compared with other kinds of pairs considered and also with isolated tetrahedral hydrogen atoms. The connection with the electronic structure of the system is also examined.

I. INTRODUCTION

When a metal absorbs hydrogen, a variety of interesting phenomena exists over an extended range of hydrogen concentration. The disordered and low-concentration solid solution (α phase) is of particular interest. Some unique characteristic features exist in some of the hexagonal close-packed (HCP) metals such as Sc, Y, and heavy rare earths (Ho, Er, Tm, and Lu). The most interesting one is the peculiar phase boundary independent of temperature from nearly 400 K down to very low temperature, which has been observed in α-$LuH(D)_x$,[1–3] α-$TmH(D)_x$,[2–4] α-$YH(D)_x$,[2,5] and α-$ErH(D)_x$.[2,3] This is in contrast to the almost vanishing solubility of hydrogen at low temperature in other metals. An electrical resistivity anomaly around 150–180 K (Ref. 6) has also been reported for the hydrogen (deuterium) solid solutions in Lu,[7,8] Sc,[9,10] Er,[11] Y,[12] and Tm.[13] An understanding of the nature of these anomalies in the phase diagram and in resistivity has been the subject of many experimental and theoretical studies.

In α-YH_x hydrogen remains in solution up to a critical concentration of $x = [H]/[Y] = 0.245$ (Ref. 5) and a resistivity anomaly was observed around 168 K.[5] From various experimental results, a microscopic picture of this anomaly in the solid solution has been gradually established. The argument sets in that certain ordering patterns of hydrogen atoms are formed in the seemingly disordered solid-solution phase. Neutron diffraction[14] showed that hydrogen atoms occupy tetrahedral sites almost exclusively. As the material is cooled down from high temperatures, hydrogen starts forming pairs (short-range ordering) bridged by the metal atoms with a separation of $3c_0/4$ along the c axis.[5,15] Subsequently, when the temperature becomes even lower, these pairs tend to arrange themselves into lines and chains (long-range ordering) along the c axis.[16–19]

Diffuse neutron-scattering measurements by McKergow *et al.*[17] for α-$YD_{0.17}$ found scattering intensity ridges in a plane normal to the c^* direction near (0,0,4/3), indicating that deuterium forms pairs on the next-nearest tetrahedral sites along the c direction with a yttrium atom in between. These intensity ridges became stronger and narrower and moved closer to (0,0,4/3) as temperature was decreased. In order to account for this feature, a model in which these pairs order linearly along the same c axis [see Fig. 1(a)] was proposed.[17] Later the correlation of pairs along the basal directions was considered based on a recent diffuse neutron-scattering measurement of $YD_{0.1}$.[18] Figure 1(b) gives a sketch of the latest model where two adjacent lines of hydrogen pairs form a zigzag chain. The projection onto the vertical direction has a $3c_0/4$ periodicity in the real space. This correlation in the basal plane has a better agreement with the observed modulation of the intensity ridge perpendicular to c^* (Ref. 18) and is in agreement with the model proposed earlier for α-LuD_x (Ref. 20) and α-ScD_x.[21]

This high degree of order at low temperature leads to the so-called α^* phase which is distinguished from the disordered (or partially ordered) α phase at higher temperatures. These orderings, short-range or long-range, are believed to be the origin of the anomalous terminal solubility. Little is known, however, about the fundamental mechanism which induces these unique H orderings. Some researchers[17,18] explained it from the picture of charge density waves while some[20] ascribed it to the formation of coherent stresses within the metal lattice. The nuclear magnetic resonance (NMR) measurements of the proton spin-lattice relaxation rate in α-ScH_x (Ref. 22) revealed an electronic structure change near 170 K, which was in the same temperature range where the resistivity anomaly occurred. Previous theoretical studies of the pairing were performed either for small clusters[23] within the local density approximation

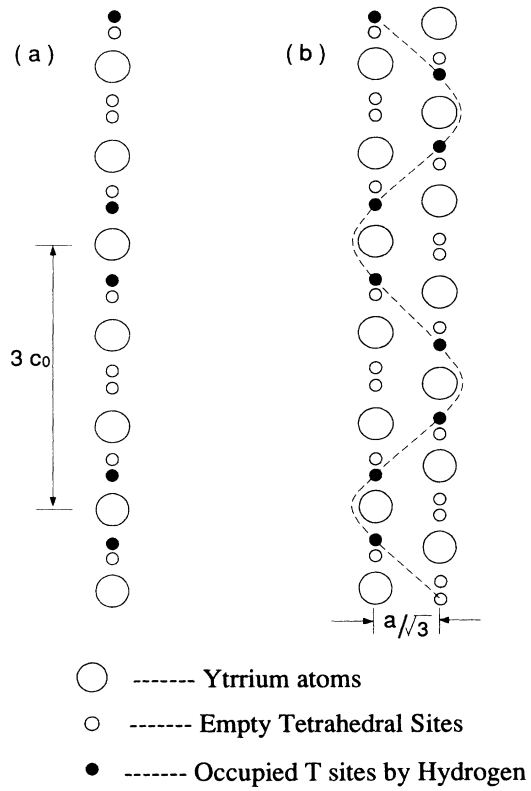

FIG. 1. Two hydrogen ordering models in the solid solution: (a) hydrogen pairs order linearly along the c axis; (b) correlated linear chain.

(LDA) (Ref. 24) or for a crystal using supercells and the extended Hückel method.[25] Both agreed on the occupation of tetrahedral sites, but disagreed on the pairing energy and configuration. The cluster calculation[23] found that hydrogen atoms paired across a metal atom, while the extended Hückel calculation[25] found that other pairs were more energetically favorable and stable.

In addition to the pairing problem, the inelastic neutron-scattering measurements[15,26] observed nondegenerate local vibrational frequencies for H, an indication of the existence of an anharmonic hydrogen potential in this system. The dynamical properties of H in α-YH_x have hence aroused much interest. A recent LDA pseudopotential mixed-basis calculation[27,28] reported the potential-energy surface of hydrogen in hypothetic $YH_{0.5}$.

In this paper, a self-consistent pseudopotential total-energy calculation is carried out to study a variety of properties of the hydrogen solid solution in HCP yttrium. The (pseudo)wave functions are expanded with the plane-wave basis. Ordered structures of different concentrations ($YH_{0.5}$, $YH_{0.25}$, $YH_{0.167}$) are examined using the supercell method. The tetrahedral sites are found to be always lower in energy than the octahedral sites. From an adiabatic hydrogen potential in $YH_{0.25}$, a local vibrational mode of H atom along the c axis is found to be of 100 meV, in excellent agreement with experimental measurements. In particular, the issue of hydrogen ordering (pairing) is addressed from this first-principles calculation. The formation of hydrogen pairs at the tetrahedral sites bridged by an yttrium atom is found to be energetically favorable. The mechanism of this pairing is examined from the electronic structure and individual components of the total energy.

The paper is organized as follows. The calculational details are first presented in Sec. II. All the results are included in Sec. III, where the binding energies for various hydrogen compositions and different interstitial sites are given in Sec. III A, hydrogen potential curves are examined in Sec. III B, and the investigation related to hydrogen pairing is presented in Sec. III C. Finally the major results of this work are summaried in Sec. IV.

II. CALCULATIONAL TECHNIQUES

Elemental yttrium is in the HCP structure with a c/a ratio slightly less than the ideal value of $\sqrt{8/3}$ by 3%. The measured lattice constants[29] are $a = 3.65$ Å and $c/a = 1.57$. A conventional unit cell in this structure is indicated by a highlighted box shown in Fig. 2. In the calculation the origin is chosen at an octahedral site in order to utilize the inversion symmetry of the system. There are two different kinds of interstitial sites in this structure: tetrahedral (T) and octahedral (O) sites which are also illustrated in Fig. 2.

With the development of "soft" pseudopotentials[30] it has been possible to perform *ab initio* pseudopotential calculations for transition metals using a plane-wave basis. A detailed study on the structural properties of HCP yttrium[31] has been performed and good convergence was achieved with an energy cutoff of 36 Ry for this early transition metal element. A correction[32] was included for the exchange-correlation energy due to the valence-core charge overlap. Various structural properties obtained were in good agreement with experimental values. The pseudopotential for hydrogen is also generated by using the same scheme from atomic configuration $1s^1$ with a

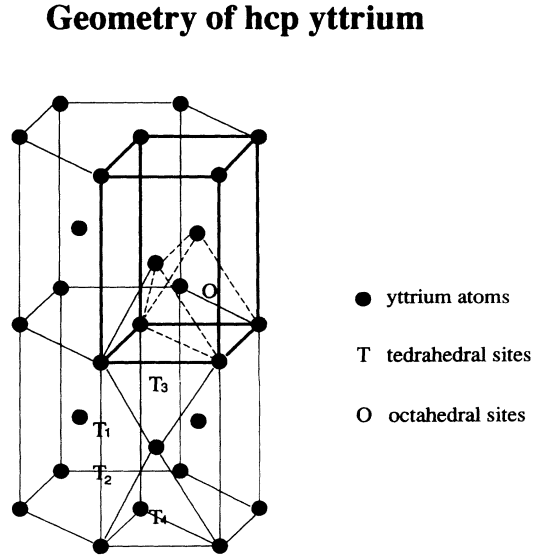

FIG. 2. Hexagonal close-packed structure. The interstitial sites are marked.

radial cutoff of 0.88 a.u. for the s orbital. The motivation for doing so is to avoid poor convergence introduced by the $1/r$ ionic hydrogen potential. With a full HCP symmetry, 36 k points are used in the irreducible Brillouin zone (correspond to 648 distinct reducible vectors in the full zone). This number varies in the supercell modeling. A Gaussian smearing method[33] with a width of 0.1 eV is employed to accelerate the convergence of the total energy with respect to the number of k points. The s potential has been chosen as the local potential in the calculation and the Wigner correlation formula[34] is used.

The hydrogen solid solution phase is examined at several hydrogen concentrations. The supercell method is used to model the system with different concentrations and to preserve the periodicity of the system. A system with a lower concentration requires a larger unit cell. The binding energies of the two different kinds of interstitial sites are also studied. Three hydrogen compositions with $x = 0.5$, 0.25, and 0.167 are covered in this work, which correspond to a single, double, and triple cell modeling. The hypothetic composition of 0.5 is the simplest case where each unit cell accommodates only one hydrogen (Y_2H_1). For the compositions of 0.25 and 0.167, the dimension of the unit cell is increased along the hexagonal axis which leads to an ordered structure of Y_4H_1 and Y_6H_1 respectively. The number of plane waves included in each calculation is 1000, 3000, and 6000 respectively. Later the pairing problem is investigated in the triple cell with a composition of Y_6H_2.

The comparison of the individual components of the total energy among different configurations provides a valuable tool in analyzing and understanding the properties of the system. The total energy is given by[35]

$$E_{\rm tot} = E_{\rm kin} + E_{\rm ec} + E_H + E_{\rm xc} + E_{\rm cc} + E_\alpha. \qquad (1)$$

The individual contributions here are the electronic kinetic energy, the electron-core interaction energy which comes from both the local and nonlocal potential energies, the electron-electron Hartree energy, the exchange-correlation energy, and the core-core Coulomb (Ewald) energy, respectively. The last term, E_α, results from the deviation of the pseudopotential from $1/r$ in the core region.[35]

III. RESULTS AND DISCUSSIONS

A. Energetics

First the global lattice relaxation due to the presence of hydrogen is considered. The equilibrium volume for the ordered structure $YH_{0.25}$ and $YH_{0.5}$ is determined with one hydrogen occupying the tetrahedral site in the proper unit cell respectively. The total energy is minimized with respect to both the volume and c/a ratio. The equilibrium volumes are obtained from the fitting to Murnaghan's equation of state[36] and the results are listed in Table I. It is found that the equilibrium values for $YH_{0.25}$ ($YH_{0.5}$) are 435 (447) a.u.^{3} in volume and 1.60 (1.62) in the c/a ratio. Comparing with the calculation for elemental HCP yttrium, a volume expansion of 3% (6%) is found and the c/a ratio is increased by about 2% (3%). The experimental values[2] for $YH_{0.19}$ correspond to a 2% and 0.6% expansion for volume and the c/a ratio respectively. If it is assumed that the lattice constants increase linearly with hydrogen concentration from YH_0 to $YH_{0.5}$, our results would be consistent with experiment in the volume expansion, yet the theoretical c/a ratio seems to be larger. Nevertheless, it is found that the calculated total energy is quite insensitive to the variation of the c/a ratio. A typical variation in the total energy as c/a changes from 1.57 to 1.62 is about 0.1 mRy/atom. As a result, the difference in the c/a ratio between the calculated and measured values should not affect the calculated properties substantially. For subsequent calculations with other hydrogen concentrations $x < 0.5$, both the volume and c/a ratio were estimated from a linear interpolation between $YH_{0.5}$ and pure yttrium YH_0.

TABLE I. Equilibrium lattice parameters for YH_x.

Configuration	Volume (a.u.^{3})	c/a
$YH_{0.0}$	420.8	1.56
$YH_{0.25}$	434.8	1.60
$YH_{0.5}$	447.1	1.62
Experiment		
$YH_{0.0}$	446[a]	1.57[a]
$YH_{0.19}$	456[b]	1.58[b]

[a]Reference 29.
[b]Reference 2.

The binding energy per hydrogen is defined as

$$E_b = \tfrac{1}{x}\left[E(YH_x) - E(Y_{\rm metal})\right] - E(H_{\rm atom}), \qquad (2)$$

which is referenced to the energy of atomic hydrogen (−13.6058 eV). The binding energies of hydrogen for various hydrogen concentrations and different interstitial sites are calculated. The results are listed in Table II. Since the values for $YH_{0.25}$ and $YH_{0.167}$ differ by only 0.01 eV per H atom, it is expected that the binding energy for the system with a smaller concentration (which requires a larger supercell in the calculation) will not change significantly. Note that the local relaxation effect is not included in the calculation, hence the values in Table II are in fact upper bounds. It is found that the tetrahedral site has a lower energy (about 110 meV) than the octahedral site. The energy difference is

TABLE II. Binding energy of hydrogen (eV per atom) in yttrium as defined in Eq. (2) for various concentrations in the α phase.

	Tetrahedral (T)	Octahedral (O)
$YH_{0.50}$	−2.84	−2.67
$YH_{0.25}$	−2.80	−2.69
$YH_{0.167}$	−2.79	

TABLE III. Comparison of various energy contributions to the total energy per cell (Y_4H) between hydrogen occupying the tetrahedral (T) and octahedral (O) sites. The energy terms are given in Eq. (1).

	T (Ry)	O (Ry)	Difference (eV)
E_{tot}	−19.505	−19.497	−0.110
E_{kin}	11.756	11.681	1.016
E_{ec}	−11.451	−11.098	−4.801
E_H	0.731	0.599	1.797
E_{xc}	−12.571	−12.520	−0.692
E_{cc}	−17.796	−17.985	2.572
E_α	9.826	9.826	0.0

much smaller than that found in the cluster calculation[23] and the extended Hückel calculation,[25] but consistent with previous pseudopotential mixed-basis calculations for $YH_{0.5}$,[27,28] in which the zero-point energy was also estimated. The inclusion of the zero-point energy will not change the order of the energy between the two sites. Hence the occupation of tetrahedral sites is energetically more favorable. This is consistent with the conclusion of neutron-scattering experiments.[16]

The difference in individual energy contributions is examined when hydrogen occupies the tetrahedral and octahedral sites at $x = 0.25$: $YH_{0.25}(T)$ and $YH_{0.25}(O)$. Various energy terms are shown in Table III. From the energy differences [the energy of $YH_{0.25}(T)$ subtracted by that of $YH_{0.25}(O)$], it clearly shows that the kinetic energy E_{kin}, Hartree energy E_H, and Ewald energy E_{cc} all favor the octahedral site, while the exchange-correlation energy E_{xc} and electron-core interaction term E_{ec} are lowered when hydrogen occupies the tetrahedral site. The occupation of the tetrahedral sites leads to a smaller nearest-neighbor hydrogen-metal distance for a fixed volume. This smaller hydrogen-metal distance gives rise to a more compact valence charge distribution. Thus, E_{kin} and E_H increase while E_{ec} decreases. The Ewald contribution, however, increases because of the larger electrostatic potential energy between neighboring atomic cores, but it is balanced by the electronic terms. It is noticed that the major lowering in energy in $YH_{0.25}(T)$ is from E_{ec} and a further decomposition of it shows that the local potential (s) contribution is responsible. Apparently, hydrogen occupies the tetrahedral site in order to optimize the interaction of the proton and surrounding electrons. The density of states in $YH_{0.25}$ reveals the presence of H-induced states at about 5 eV below the Fermi level. This is in agreement with the photoemission results.[37]

B. Hydrogen vibration and diffusion

The adiabatic hydrogen potentials can be obtained through the computation of the total energy repeatedly by displacing H in the metal lattice. The dynamical properties of hydrogen in the α phase have been studied by the pseudopotential mixed-basis method for hypothetic $YH_{0.5}$ in the adiabatic approximation.[28] Here we extend the study to lower concentration to examine the dependence on concentration. In this section, the hydrogen potential curves around the tetrahedral sites along the c axis ($T-T$) and along the path connecting the adjacent octahedral and tetrahedra sites ($O-T$) are examined in particular.

First the local vibrational frequency along the c axis is calculated from the potential energy curve for $x = 0.25$ (Y_4H_1). Total energies are evaluated with H located at six equally spaced points, as shown in Fig. 3. Then the calculated potential energies are fitted with an even-order polynomial up to the fourth order. The results are presented in Fig. 3. The solid circles are the calculated values with number 4 being the potential energy of the tetrahedral site and the solid line is from the fitting. The minimum energy is chosen as the energy reference. It

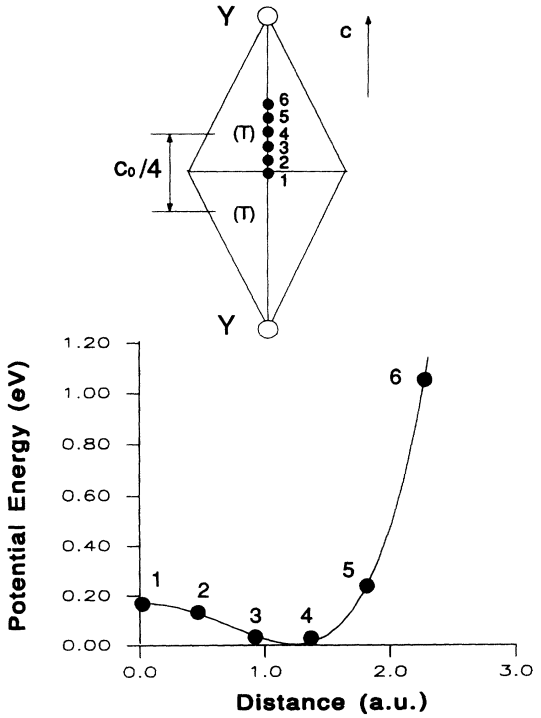

FIG. 3. The calculated (solid circles) and fitted (solid line) potential well for hydrogen moving along the c axis for $YH_{0.25}$. The six points used in the calculation are labeled with number 4 being the tetrahedral site.

can be seen that the potential well is anharmonic with the position of the minimum slightly shifted from the exact tetrahedral position, consistent with experimental findings.[15,26] Furthermore, a barrier of about 170 meV between the two adjacent tetrahedral sites is found. This calculated barrier should be an upper limit since metal relaxation is not considered in the total energy calculation. Considering this as a one-dimensional quantum system, a set of eigenvalues are obtained by solving the Schrödinger equation for the proton in this double-well potential. A list of these eigenvalues is shown in Fig. 4. The energy difference between the ground and first excited states is found to be around 100 meV, which is in good agreement with the energy of the local mode observed in the inelastic neutron scattering.[26] In addition, the same calculation is performed for Y_2H_1 ($x = 0.5$) to check the concentration dependence. It was found that the height of potential barrier is about 178 meV and the local vibrational mode also about 100 meV. In comparison, the dependence of the general features of the potential well and local vibrational mode on H concentration is not significant. We have also calculated the potential-energy curve along the diffusion path connecting the adjacent tetrahedral and octahedral sites for $YH_{0.5}$. A barrier of 0.5 eV is found which is in excellent agreement with the activation energy measured from the NMR spin-lattice relaxation time[38] and the result of the mixed-basis calculation.[28]

C. Hydrogen pairing

In order to study the hydrogen ordering along the c axis, the conventional HCP unit cell is tripled along the hexagonal axis with its dimension on the ab plane remaining the same. This cell consists of six yttrium atoms. Two tetrahedral H atoms are arranged to form various pairing configurations. This leads to a hydrogen composition of $YH_{0.33}$ (Y_6H_2) with the volume and c/a ratio obtained by a linear interpolation from the results of $YH_{0.5}$ and YH_0. The lattice constants from the fitting are $a = 3.60$ Å and $c \simeq 3c_0 = 17.29$ Å. Four different pairing configurations within the triple cell are investigated, as shown in Fig. 5, where the large open circles indicate the yttrium atoms and the smaller solid (open) circles are the occupied (unoccupied) tetrahedral sites. Configuration (I) is formed by placing two H atoms at nearest-neighbor tetrahedral sites (e.g., T_1 and T_2 in Fig. 2) with a separation of $d_1 = c/12 = 1.44$ Å , while (II), (III), and (IV) correspond to pairs at larger distances. In both (III) and (IV) hydrogen pairs order linearly along the c axis with the hydrogen-hydrogen distance being $d_3 = c/3 = 5.76$ Å and $d_4 = c/4 = 4.32$ Å (e.g., T_3 and T_4 pair in Fig. 2), respectively. All these linearly ordered pairs are apart from each other horizontally by the lattice constant a. The pairing configuration (II), in which the pairs do not follow the linear pattern along c, is also considered since the separation of the two H in this pair is small: $d_2 = 0.702a = 2.53$ Å (e.g., T_1 and T_3 pair in Fig. 2) and the energy for this pair was found relatively low by a previous extended Hückel calculation.[25] The number of symmetry operations has been reduced from 24 to 6 due to the way the tetrahedral sites are occupied. The number of plane waves is about 6000.

The total energy is first calculated for each of the pairing configurations. The energy per pair, which is defined as

$$E_{\text{pair}} = E(Y_6H_2) - 6E(Y_{\text{bulk}}) - 2E(H_{\text{atom}}), \qquad (3)$$

is listed in Table IV. The energy for the nearest-neighbor

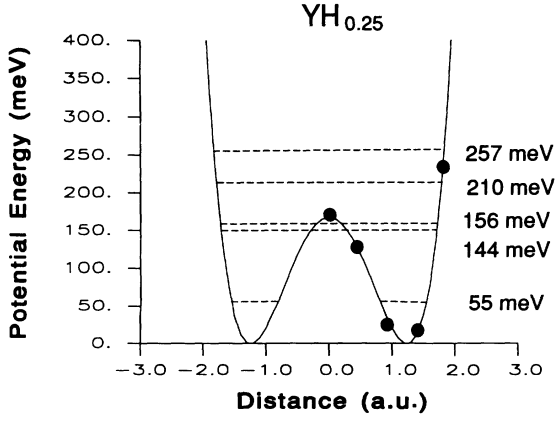

FIG. 4. A few estimated eigenvalues for hydrogen vibration in the double-well potential along the c axis. The lowest energy has two states very close to each other.

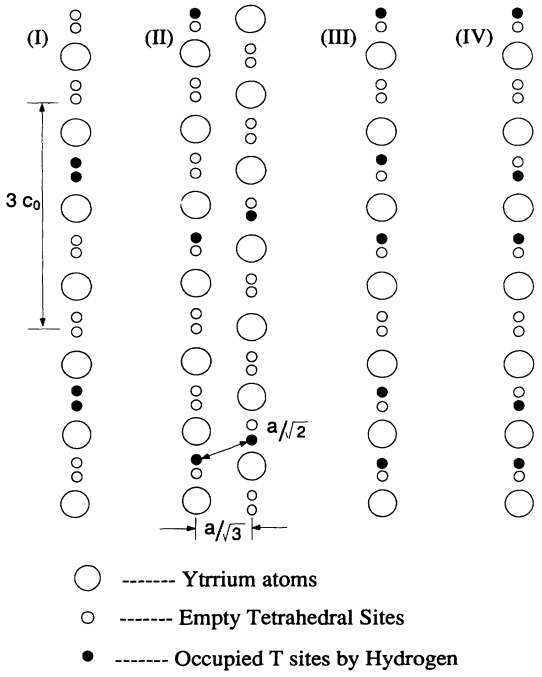

FIG. 5. Various pairing configurations along the c axis used in the calculations. The large open circles are the yttrium atoms and the small open circles are the unoccupied tetrahedral sites while the solid ones are the occupied tetrahedral sites by hydrogen atoms. The distance between the two H atoms in configuration (II) is labeled by assuming an ideal c/a ratio.

TABLE IV. Comparisons of the pairing energy (eV per pair) defined in Eq. (3), the total energy and the individual energy (both in Ry per Y_6H_2) among various pairing configurations as defined in the text. All the results are obtained from the triple cell calculations.

Configurations	(I)	(II)	(III)	(IV)
Distance (Å)	1.44	2.53	5.76	4.32
Pairing energy	−4.97	−5.56	−5.63	−5.68
$E_{\rm tot}$	−29.815	−29.859	−29.864	−29.868
$E_{\rm kin}$	18.354	18.187	18.146	18.167
$E_{\rm ec}$	−21.686	−21.318	−18.384	−19.118
E_H	3.021	2.912	1.461	1.818
$E_{\rm xc}$	−19.252	−19.236	−19.236	−19.239
$E_{\rm cc}$	−25.369	−25.520	−26.968	−26.612
E_α	15.117	15.117	15.117	15.117

tetrahedral site pairs (I) is −4.97 eV per pair and is much higher than that of other pairs. The possibility of pairing in this configuration, hence, can be ruled out. This is in accordance with the minimum distance criterion proposed by Switendick.[39] Hydrogen pairing on adjacent tetrahedral sites bridged by a yttrium atom along the c axis, configuration (IV), gives the lowest energy. This energy is about 710 meV, 120 meV, and 50 meV per pair lower than that of pairing configurations (I), (II), and (III), respectively. The binding energy for configuration (IV) is found to be −2.84 eV per hydrogen according to Eq. (1), which is lower than the estimated binding energy of isolated hydrogen atoms, −2.79 eV (Table II). Therefore, pairing of hydrogen across a metal atom is indeed energetically favorable compared with other pairing configurations and isolated atoms, which fully supports the experimental observations. The previous cluster calculation[23] gave a similar pairing energy for configuration (IV). However, the absolute binding energy was quite different in small clusters.

Besides the total energy, various energy contributions to the total energy (see Table IV) are also analyzed in order to understand the difference between various pairing configurations. The very high Ewald energy in configuration (I), due to the small hydrogen-hydrogen distance, contributes to the unstability in this configuration as expected. The configurations of (III) and (IV) are compared more closely, in particular, to understand the mechanism of the preferential pairing configuration (IV). It is found that the electron-core contribution $E_{\rm ec}$ is lowered by moving one of the two hydrogens per triple cell to form the pairing configuration (IV). A further decomposition to $E_{\rm ec}$ gives that more than 90% in this decrease comes from the local (s) potential energy. This will be further analyzed below.

The electronic band structure $E(\mathbf{k})$ is shown in Fig. 6 for pairing configuration (III) and compared with that for pairing configuration (IV) shown in Fig. 7. The flatness of the curves along the vertical directions (Γ-A, M-L, and H-K) is a remnant of the band structure of pure HCP yttrium and also an indication of a localized Y-H interaction along the c direction. Near the Fermi level, the

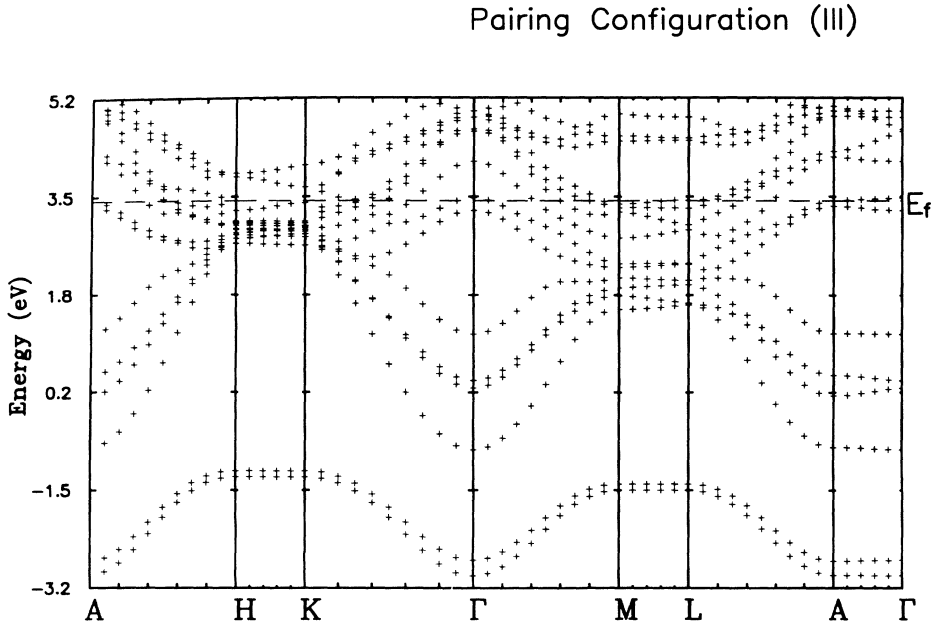

FIG. 6. The electronic band structure corresponding to pairing configuration (III) as defined in the text.

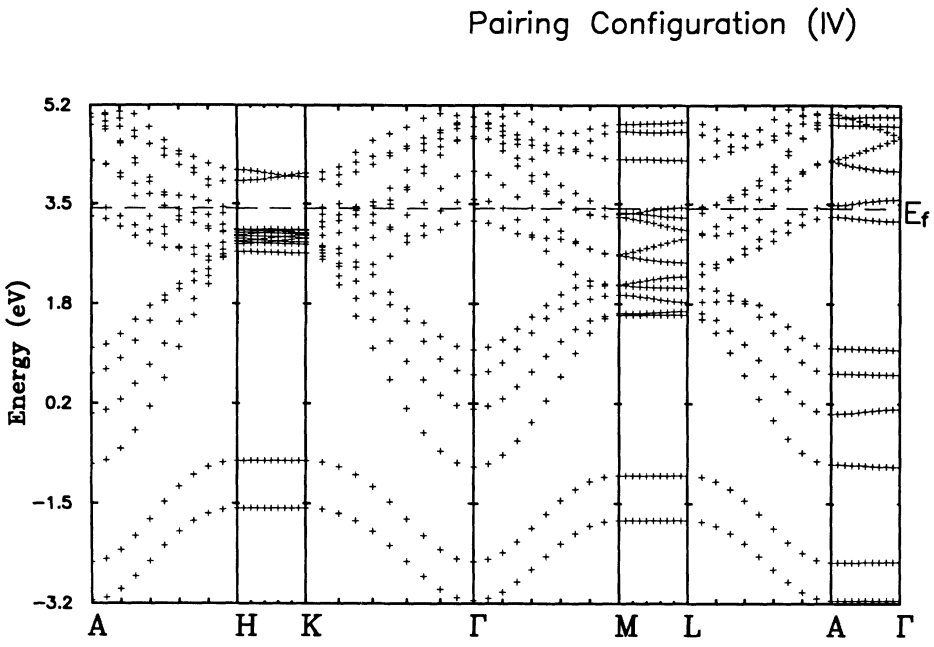

FIG. 7. The electronic band structure corresponding to pairing configuration (IV) as defined in the text.

most noticeable difference between Figs. 6 and 7 appears to be along K to H. With the formation of hydrogen pairs across a metal atom, the occupied and empty bands become well separated, which leads to a band gap of about 1 eV in this direction. Thus the lowering of the total energy is closely connected with the electronic structure.

The wave functions at K are further analyzed. In Fig. 8, the states right below and above the Fermi level are shown in (a) and (b) respectively for pairing configuration (III) and compared with those for pairing configuration (IV) in Figs. 9(a) and 9(b). The open (solid) circles represent the metal (tetrahedral H) atoms. It is these two states that have shifted significantly in energy when the pairing configuration changes from (III) to (IV) (Figs. 6 and 7). In configuration (III), these two hydrogen atoms are well separated and the wave function amplitude is

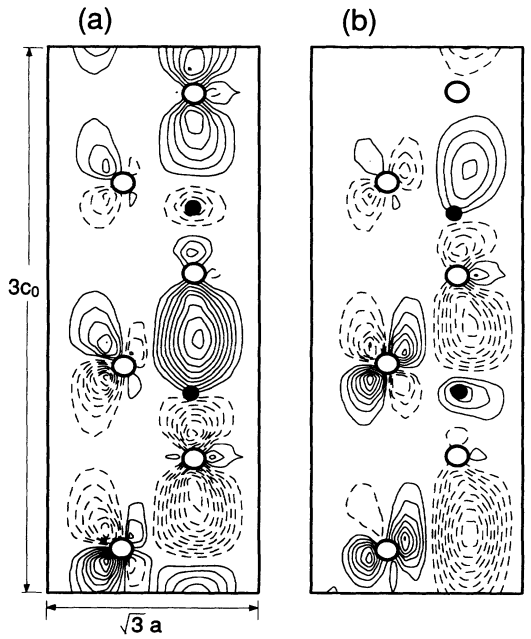

FIG. 8. Wave functions (real part) at K for pairing configuration (III) with the large open (small solid) circles indicating the positions of the metal atoms (hydrogen occupied tetrahedral sites). (a) and (b) correspond to the states right below and above the Fermi level, respectively.

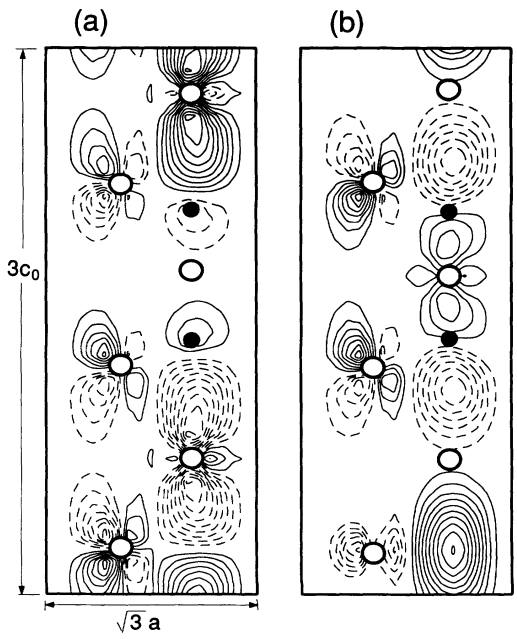

FIG. 9. Wave functions (real part) at K for pairing configuration (IV) with the large open (small solid) circles indicating the positions of the metal atoms (hydrogen occupied tetrahedral sites). (a) and (b) correspond to the states right below and above the Fermi level, respectively.

not correlated (Fig. 8). In contrast, when the pair is formed directly across the metal atom, the wave function exhibits certain symmetry as a result of the interaction (Fig. 9). In particular, the state below the Fermi level contains an antisymmetric combination of two H $1s$ orbitals with local maxima at the proton positions [see Fig. 9(a)], while the one above the Fermi level has nodes at the proton sites [Fig. 9(b)]. Thus the energy separation between them is greatly increased. This result is also consistent with the observation in the analysis of individual energy contributions above. The larger amplitude of the wave functions at the symmetric proton sites for the states below the Fermi level lowers the local (s) potential energy in configuration (IV) and thus makes the pairing configuration (IV) energetically favorable. Other bands grouped together along K to H are found to have the combination of different yttrium characteristics and are not affected very much.

Other interesting differences between the two band structures, such as the substantial change throughout the whole Brillouin zone in the separation of the first and second lowest bands, can also be understood by the analysis of wave functions. These two bands have significant H-s character with the first (second) band containing the in-phase (out-of-phase) combination of the two hydrogen wave functions. With the interaction in pairing configuration (IV), these two bands further split and become well separated.

The fact that the pairing across the metal atom [configuration (IV)] has the lowest energy and that there is a noticeable change in the electronic structure indicates that the pairing mechanism has an electronic origin. This is consistent with the finding of the NMR measurements for α-ScH_x.[22] These measurements revealed an electronic structure change at $\sim$ 170 K, where the product of the charge density at the proton sites and the electronic density of states increased by roughly 4% with decreasing temperature. This temperature range coincides with that of the resistivity anomaly, which is believed to be associated with the linear ordering of hydrogen pairs. As can be seen from the above analysis, there is indeed an increase in the charge density at the proton sites when the linear ordering takes place.

In the above total energy calculations, the metal atoms have been held fixed. Since we did not allow the metal atoms to relax, the effect of coherent stress within the metal lattice[20] on the pairing of hydrogen was not studied. We have also ignored the chainlike arrangement of these pairs [Fig. 1(b)], but the correct linear periodicity of the pairs ($3c_0$) was included. Further investigations of the planar correlation between these linearly ordered pairs require a much larger supercell and are being planned.

IV. CONCLUSION

In summary, the hydrogen solid solutions in HCP yttrium are studied by using pseudopotentials and the plane-wave basis within the local-density approximation. The binding energy at various hydrogen compositions from $x = 0.167$ to 0.5 is obtained by the supercell modeling method. It is shown that the hydrogen atoms prefer to occupy the tetrahedral sites over the whole range. From the calculated adiabatic hydrogen potential in $YH_{0.25}$ along the c axis between nearest-neighbor T sites, a strong anharmonic potential curve is obtained and a local vibrational mode is found to be about 100 meV by solving the one-dimensional Schrödinger equation. The self-consistent total energy calculation for various pairing configurations supports the experimental observations and clarifies the controversy on the pairing configuration between previous calculations. The possibility of hydrogen pairing at nearest-neighbor tetrahedral sites can be excluded due to its distinct high energy over other pair configurations. The linear ordering of pairs at tetrahedral sites bridged by a metal atom gives the lowest energy and is related to the features in the electronic structure.

ACKNOWLEDGMENTS

We would like to thank Dr. A. C. Switendick for the general discussions on the hydrogen-metal systems. This work was supported by the U.S. Department of Energy under Contract No. DE-FG05-90ER45431 and partly by the NSF. A grant for supercomputer time from the Pittsburgh Supercomputing Center (DMR890007P) is also acknowledged. M.Y.C. acknowledges the support of the Packard Foundation.

[1] J. N. Daou and J. E. Bonnet, J. Phys. Chem. Solids **35**, 59 (1974).
[2] B. J. Beaudry and F. H. Spedding, Metall. Trans. B **6**, 419 (1975).
[3] J. N. Daou and P. Vajda, J. Phys. F **12**, L13 (1982).
[4] J. E. Bonnet and J. N. Daou, J. Phys. Chem. Solids **40**, 421 (1979).
[5] J. E. Bonnet, C. Juckum, and A. Lucasson, J. Phys. F **12**, 699 (1982).
[6] For a review, see J. N. Daou and P. Vajda, Ann. Chim. Fr. **13**, 567 (1988).
[7] J. N. Daou, A. Lucasson, and P. Lucasson, Solid State Commun. **19**, 895 (1976); J. P. Burger, J. N. Daou, A. Lucasson, P. Lucasson, and P. Vajda, Z. Phys. Chem. Neue Folge **143**, 111 (1985).
[8] P. Vajda, J. N. Daou, J. P. Burger, K. Kai, K. A. Gschneider, Jr., and B. J. Beaudry, Phys. Rev. B **34**, 5154 (1986).
[9] C. L. Jensen and M. P. Zalesky, J. Less-Common Met. **75**, 175 (1980).
[10] J. N. Daou, P. Vajda, A. Lucasson, and J. P. Burger, Phys. Status Solidi A **95**, 543 (1986); J. N. Daou, P. Vajda, A. Lucasson, P. Lucasson, and J. P. Burger, Philos. Mag. A

53, 611 (1986).
[11]J. N. Daou, P. Vajda, A. Lucasson, and P. Lucasson, J. Phys. C **14**, 3155 (1981).
[12]P. Vajda, J. N. Daou, A. Lucasson, and J. P. Burger, J. Phys. F **17**, 1029 (1987).
[13]J. N. Daou, P. Vajda, A. Lucasson, and P. Lucasson, Solid State Commun. **38**, 135 (1981); J. Phys. C **14**, 129 (1981).
[14]D. Khatamian, C. Stassis, and B. J. Beautry, Phys. Rev. B **23**, 624 (1981).
[15]I. S. Anderson, J. J. Rush, J. Udovic, and J. M. Rowe, Phys. Rev. Lett. **57**, 2822 (1986).
[16]J. E. Bonnet, D. K. Ross, D. A. Faux, and I. S. Anderson, J. Less-Common Met. **129**, 287 (1987).
[17]M. W. McKergow, D. K. Ross, J. E. Bonnet, I. S. Anderson, and O. Schaerpf, J. Phys. C **20**, 1909 (1987).
[18]J. P. A. Fairclough and D. K. Ross (unpublished).
[19]O. Blaschko, J. Less-Common Met. **172**, 174 (1991).
[20]O. Blaschko, G. Krexner, J. N. Daou, and P. Vajda, Phys. Rev. Lett. **55**, 2876 (1985); O. Blaschko, G. Krexner, L. Pintschkovius, G. Ernst, P. Vajda, and J. N. Daou, Phys. Rev. B **39**, 5605 (1989).
[21]O. Blaschko, L. Pintschkovius, P. Vajda, J. P. Burger, and J. N. Daou, Phys. Rev. B **40**, 5344 (1989).
[22]L. Lichty, J. W. Han, R. Ibanez-Meier, D. R. Rorgeson, R. G. Barnes, E. F. W. Seymour, and C. A. Sholl, Phys. Rev. B **39**, 2021 (1989).
[23]Feng Liu, M. Challa, S. N. Khanna, and P. Jena, Phys. Rev. Lett. **63**, 1369 (1989); **65**, 1169 (1990).
[24]P. Hohenberg and W. Kohn, Phys. Rev **136**, B864 (1964); W. Kohn and L. J. Sham, *ibid.* **148**, A1133 (1965).
[25]C. Minot and C. Demangeat, Z. Phys. Chem. Neue Folge **549**, 163 (1989); C. Koudou, C. Minot, and C. Demangeat, Phys. Rev. Lett. **64**, 1474 (1990).
[26]I. S. Anderson, N. F. Berk, J. J. Rush, and T. J. Udovic, Phys. Rev. B **37**, 4358 (1988).
[27]B. J. Min and K. M. Ho, Phys. Rev. B **40**, 7532 (1989).
[28]B. J. Min and K. M. Ho, Phys. Rev. B **45**, 12 806 (1992).
[29]B. J. Beaudry and K. A. Gschneidner, Jr., in *Handbook on the Physics and Chemistry of Rare Earths,* edited by K. A. Gschneidner, Jr. and L. R. Eyring (North-Holland, Amsterdam, 1978).
[30]N. Troullier and J. L. Martins, Phys. Rev. B **43**, 1993 (1991).
[31]Y. Wang and M. Y. Chou, Phys. Rev. B **44**, 10 339 (1991).
[32]S. G. Louie, S. Froyen, and M. L. Cohen, Phys. Rev. B **26**, 1738 (1982).
[33]C. L. Fu and K. M. Ho, Phys. Rev. B **28**, 5480 (1983).
[34]E. Wigner, Phys. Rev. B **46**, 1002 (1934).
[35]J. Ihm, A. Zunger, and M. L. Cohen, J. Phys. C **12**, 4409 (1979).
[36]F. D. Murnaghan, Proc. Natl. Acad. Sci. U.S.A. **30**, 244 (1944); O. L. Anderson, J. Phys. Chem. Solids **27**, 547 (1966).
[37]J. H. Weaver, D. T. Peterson, R. A. Butera, and A. Fujimori, Phys. Rev. B **32**, 3562 (1985).
[38]L. Lichty, R. J. Schoenberger, D. R. Torgeson, and R. G. Barnes, J. Less-Common Met. **129**, 31 (1987).
[39]A. C. Switendick, Z. Phys. Chem. Neue Folge **117**, 89 (1980).